EIR-Bericht Nr. 544
Februar 1985

EIR-Bericht Nr. 544

Februar 1985

An Axial Calculation Method for Accurate Two-Dimensional PWR Core Simulation

P. Grimm

Eidgenössisches Institut für Reaktorforschung
Institut Fédéral de Recherches en Matière de Réacteurs
Swiss Federal Institute for Reactor Research

CH-5303 Würenlingen Tel. 056 99 21 11 Telex 53 714 eir ch

EIR-Bericht Nr. 544

AN AXIAL CALCULATION METHOD FOR ACCURATE TWO-DIMENSIONAL PWR CORE SIMULATION

P. Grimm

Abstract

An axial calculation method, which improves the agreement of the multiplication factors determined by two- and three-dimensional PWR neutronic calculations, is presented. The axial buckling is determined at each time point so as to reproduce the increase of the leakage due to the flattening of the axial power distribution and the effect of the axial variation of the group constants of the fuel on the reactivity is taken into account. The results of a test example show that the differences of k-eff and cycle length between two- and three-dimensional calculations, which are unsatisfactorily large if a constant buckling is used, become negligible if the results of the axial calculation are used in the two-dimensional core simulation.

Contents

1. Introduction

In normal operation the core of a pressurized water reactor (PWR) is free of control rods and there is no void in the coolant. Therefore, PWR's are rather homogeneous in the axial direction and the core can be calculated, e.g. for fuel management purposes, in two dimensions instead of three dimensions. The two-dimensional calculations are much cheaper than the 3-D ones and the difference in accuracy should be tolerable. However, several parametere, such as power, exposure, and water density, which the few-group cross sections of the homogenized fuel assemblies depend on, vary in the axisl direction. Therefore, it is not guaranteed that the two-dimensional calculations yield the same results (e.g. for k-eff) as the three-dimensional core simulation. In the next chapter it will be shown that the accuracy of a two-dimensional calculation which considers the third dimension simply by the geometric buckling is not satisfactory. This report presents a method by which a good agreement of k-eff between 2-D and 3-D calculations can be obtained and whose computing cost is only a small fraction of that of the 2-D calculation.

2. Problem Description

The axial power distribution in a PWR has a cosine shape in an entirely fresh core only and flattens in the course of burnup. In a typical reload core only one quarter or one third of the fuel assemblies are fresh, therefore the average axial power distribution is flatter than a cosine function even at the beginning of a cycle.

In a flatter power distribution the power density at the lower and upper edges of the core is higher and therefore the axial leakage is greater than for a cosine distribution. As a consequence, the multiplication factor k-eff is overestimated if the geometric buckling (i.e. $(\pi/H_{ex})^2$) is used in the two-dimensional calculations for a reload core. Moreover, as the axial power distribution flattens during a cycle, the axial leakage increases. Therefore the decrease of the critical boron concentration is too slow in a two-dimensional calculation with a constant axial buckling (even if the buckling is adjusted at the beginning of cycle) and hence such calculations overpredict the cycle length (i.e. the burnup at which the critical boron concentration becomes zero).

The axial variation of power and exposure has a further effect on the multiplication factor of the 2-D calculations. In the 2-D core simulation axially averaged values of these variables are used for the determination of the cross sections of each fuel assembly. If the dependence of the cross sections on power and exposure is linear (at least for the exposure, this is a good approximation) this corresponds to a volume-weighted axial average of the cross sections. However, for a proper averaging of the group constants flux-volume weighting should be used. At the axial ends of the core the flux is small and the k_∞ of the fuel is high because the power and the expoaure are small. In the middle of the core k_∞ is low and the flux is high. This is illustrated in Figure 1 which shows typical axial distributions of power and k_∞ in a PWR core (from a 1-D axial calculation). From the above considerations it follows that the k_∞ determined from the flux-weighted cross sections is smaller than the

one from the cross sections calculated with axially averaged variable values. Like the buckling problem this effect results in an overprediction of k-eff of a PWR by two-dimensional calculations.

In order to compare the accuracy of two- and three-dimensional calculations and to assess the above reactivity overestimates quantitatively a study was performed by means of the EIR light water reactor simulation code SILWER (1, 2). A simplified model of a PWR, in which the water temperature and density were assumed to be constant, was simulated both in two and three dimensions (for more detail see chapter 4). The differences between the results of two- and three-dimensional calculations are to be compared with the target accuracies for reactor physics calculations given in Table I. These values were set up by an IAEA panel in 1971 (3) and are still considered to be valid.

Quantity	Target Accuracy (%)
Reactivity	
Initial Neutron Multiplication	± 0.25 - 0.5
Reactivity Life-Time	± 2 - 5
Power Distribution	
Radial, Between Assemblies	± 1 - 3
Axial, Within an Assembly	± 3 - 5

Table I Target Accuracies for Reactor Physics Calculations (from Ref. (3))

Since the axial leakage would be underestimated in the 2-D calculation if the geometric buckling were used, a buckling which

should reproduce the leakage of the 3-D calculation was determined from the average axial power distribution at the beginning of the cycle. This buckling, which exceeds the geometric buckling by 70%, was used in the 2-D core aimulation throughout the cycle. The critical horon concentrations of the two- and three-dimensional calculations at the beginning of the cycle and at an average burnup (in the cycle) of 6000 MWd/t are shown in Table II.

Burnup (MWd/t)	Critical Boron Concentration (ppm)	
	3-D	2-D
0	783	819
6000	88	152

Table II Critical Boron Concentrations in 3-D and 2-D Calculations (Constant Buckling from Power Distribution at BOC)

It can be seen that the 2-D calculations overeatimate the critical boron concentration by 36 ppm at BOC and by 64 ppm at 6000 MWd/t. For the cross sections used a change of 15 ppm in boron concentration corresponds to approximately 0.1% in k-eff. Therefore the above overestimates of the critical boron concentration correspond to an overprediction of k-eff by 0.24% at 0 MWd/t and 0.43% at 6000 MWd/t. These values are comparable with the target accuracy for the multiplication factor (see Table I) and therefore not satisfactory, because there are several other causes which contribute to the overall error in k-eff. The cycle length (or reactivity life-time) is considerably overpredicted by the two-dimensio al calculation with a constant buckling: a linear extrapolation of .he figures in Table II

shows that a zero critical boron concentration is reached at about 6800 MWd/t in the 3-D calculation and at approximately 7400 MWd/t in the 2-D case. This is a 9% overestimate of the reactivity life-time, which is clearly beyond the target accuracy. These results show that the axial buckling must be carefully determined and reevaluated at each burnup step to account for the continuing flattening of the axial power distribution.

In an attempt to improve the results of the two-dimensional calculations a separate one-dimensional axial SILWER calculation was performed. Radially averaged exposure values were given by input at the beginning of the cycle; then a burnup calculation up to 6000 MWd/t was performed using the power distribution from the 1-D calculation in each time step. The axial bucklings were determined from the outgoing currents at the lower and upper core boundaries and the core average fluxes and diffusion coefficients (the formula is derived in section 3.4) at 0 and 6000 MWd/t. The critical boron concentrations determined with these bucklings are given in Table III, for comparison the values of the 3-D calculation are given once more.

Burnup (MWd/t)	Critical Boron Concentration (ppm)	
	3-D	2-D
0	783	829
6000	88	135

Table III Critical Boron Concentrations in 3-D and 2-D Calculations (Bucklings from Axial Calculation)

With these bucklings the difference between 3-D and 2-D calculations is practically constant and corresponds to approximately 0.3% in k-eff. This remaining overestimate is due to the difference between flux-volume weighted cross sections and cross sections calculated at axially averaged parameter values, as the following one-group consideration shows: The volume-weighted average value of the axial k_∞ distribution (from the axial calculation) shown in Figure 1 is 1.0829 and the k_∞ calculated from the interpolation formula for axially averaged power and exposure values is 1.0827. With the axial power distribution of Figure 1 as a weighting function, however, the average k_∞ reduces to 1.0796. The good agreement between the former two values shows that the assumption of a linear dependence of the cross sections on power and exposure is reasonable. The power-weighted average k_∞ is 0.3% smaller than the volume-weighted one; this difference has the same magnitude as the overprediction of k-eff by the two-dimensional calculations.

It can be concluded from the results of this example that a good agreement of k-eff (or the critical boron concentration) between two- and three-dimensional core simulations can be obtained if the axial buckling is determined (e.g. from an axial calculation) so that the axial leakages of both calculations become equal and if the effect of the difference between flux-weighted cross sections and those calculated with axially averaged parameter values is taken into account. If the critical poison density is determined in the 2-D calculations, this latter effect can be taken into account by adjusting the target eigenvalue for the boron concentration search. For the user's comfort the axial calculation should be carried out

simultaneously with the two-dimensional calculations and require as little input work as possible and no manual evaluation. The procedures chosen and implemanted in SILWER are described in the next chapter.

3. Calculation Methods

3.1 Notation

For the theoretical description of the calculation methods in the subsequent sections we introduce the following notation:

a) Symbols

B^2	Buckling (cm^{-2})
D	Diffusion coefficient (cm)
E	Exposure (MWd/t) (To avoid confusions, "exposure" shall denote the total energy released from a certain volume of fuel since its first loading into the reactor divided by the mass of uranium (in fresh state) in this volume, whereas the term "burnup", if used as a quantity in MWd/t, means the total energy produced by the reactor since the beginning of a cycle divided by the mass of uranium in the core)
H	Height of the active reactor core (cm)

J^{net} Net outgoing current through a core boundary (neutrons/$cm^2 \cdot$ sec)

k Multiplication factor (-)

L Leakage (neutrons/sec)

P Power density (MW/ton)

Q Energy per fission (Joule)

V Volume (m^3)

Δ Relative k_∞ difference (-)

Δt Length of time step in burnup calculation (days)

Δz Node height (cm)

$\bar{\rho}$ Average uranium density in the core (tons/m^3)

Σ Macroscopic cross section (cm^{-1}) (normally used with an index, not to be confused with the summation sign)

ϕ Neutron flux (neutrons/$cm^2 \cdot$ sec)

χ Fission spectrum (-)

b) Indices

a used as upper index for average cross sections: at core average variable values

f	used as upper index for average cross sections. flux-volume weighted
g,h	Energy group number
i	Mesh number in x-direction
j	" " " y-direction
k	" " " z-(axial)direction
m	Material (upper index) (denotes actually a set of interpolation formulas for the macroscopic cross sections as a function of the state variables, e.g. for a fuel assembly type or a reflector)

c) Particularities

A bar "———" indicates axial or core average values

The indices ijk refer to a three-dimensional distribution (E_{ijk},P_{ijk})

The indices ij refer to a two-dimensional distribution (P_{ij})

The index k refers to an axial distribution (P_k , Δz_k , Σ_k,...)

Cross sections:

Σ_{ag}	Absorption cross section for group g
Σ_{fg}	Fission cross section for group g
$\nu\Sigma_{fg}$	Production cross section for group g
$\Sigma_{g\to h}$	Scattering cross section from group g to group h
$\Sigma^m(x_1,x_2,..)$	Cross section (any of the above) for material m determined from the interpolation formula for the state variable values x_1, x_2,...

3.2 Exposure and Cross Section Averaging

Before the axial flux calculation can be performed, the cross sections in the one-dimensional configuration must be defined. This is not trivial for the following reasons: The few-group cross sections of the homogenized fuel assemblies depend on several state variables; typically they are given by interpolation formulas as a function of power (Doppler and xenon effects), exposure, boron concentration, and water temperature or density. Moreover, the core normally contains assemblies with different cross section sets (e.g. with different enrichments). Thus, the cross sections must be averaged at each axial node level over the fuel assemblies which have different values of the state variables and which can belong to different materials (where the term "material" is used in the sense defined in the previous section).

The best way of determining the cross sections for the axial calculation would of course be to compute the cross sections for each axial node of each fuel assembly (i.e. for a three-dimensional configuration) and to collapse them radially with the flux from the two-dimensional calculation as a weighting function. As the results of the 2-D calculation depend on the axial buckling, this would require an iteration between 2-D and axial calculations. However, the computing time and cost of the cross section determination in a three-dimensional SILWER calculation are comparable to those of the whole two-dimensional calculation. As a consequence, this method of computing the cross sections in the axial configuration would increase the cost of the two-dimensional calculations to such an extent that the 3-D core simulation would be more advantageous than the 2-D one

with regard to the ratio of computing cost and accuracy.

A simple and fast method to determine the cross sections for the axial calculation is therefore needed. The following simplifications are made in SILWER: First, we do not use flux-weighting, thus we avoid the iteration between axial and 2-D calculations. Moreover, instead of computing the cross sections for each fuel assembly with the appropriate power and exposure values and averaging them, we evaluate the interpolation formulas only once per axial node level and per material with the power density determined by the axial calculation itself and radially averaged exposures per material. The dependence of the group constants on the power density requires an iteration between cross sections and axial power distribution, whereas the exposure averaging can be performed before this iteration.

We will now describe the cross section calculation procedure used in SILWER in more detail. The cross sections are assumed to be given by interpolation formulas as a function of power, exposure, boron concentration, and water temperature for each material. Of these state variables the boron concentration (given in ppm) is constant throughout the core. The water temperature is also assumed to be constant and given by input (it would however be possible to incorporate a simplified thermohydraulic calculation into the axial calculation). The powers used for the cross section determination are those calculated in the previous iteration. The exposures however are given for each axial node of each fuel assembly, i.e. as a three-dimensional exposure distribution E_{ijk}. In the burnup calculation, which precedes the axial calculation, this exposure distribution is updated using a superposition of the 2-D and axial

power distributions:

$$E_{ijk}^{(n)} = E_{ijk}^{(n-1)} + P_{ijk}^{(n-1)} \cdot \Delta t \qquad (1)$$

with

$$P_{ijk}^{(n-1)} = P_{ij}^{(n-1)} \cdot \frac{P_k^{(n-1)}}{\bar{P}} \qquad (2)$$

Here the upper index (n) denotes the n-th time point. The exposures at the beginning of a cycle $E_{ijk}^{(0)}$ are either known from the calculation of the previous cycle or must be given by input, e.g. from integrated operating data. In the following we consider a given time point and can therefore omit the burnup step counter (n).

First the exposures are averaged in each axial node level and for each material over the fuel assemblies belonging to this material:

$$E_k^m = \frac{\sum_{ij \in m} E_{ijk} \cdot V_{ij}}{V^m} \qquad (3)$$

with

$$V^m = \sum_{ij \in m} V_{ij} \qquad (4)$$

where the subscript $ij \in m$ means that the fuel assembly at position ij in the two-dimensional configuration belongs to the material m. This exposure averaging is performed at the beginning of the axial calculation, before the iterations. Next the cross sections per material and per axial node are determined from the interpolation formulas:

$$\Sigma_k^m = \Sigma^m (P_k, E_k^m) \tag{5}$$

As the boron concentration and the water temperature are constant throughout the core we have omitted them from the argument list on the right hand side of eq. (5). Finally the cross sections are averaged over the materials for each axial node:

$$\Sigma_k = \frac{\sum_m \Sigma_k^m \cdot V^m}{\sum_m V^m} \tag{6}$$

For the calculation of the k-eff correction (see section 3.4) the cross section values at core average variable values are needed. For this purpose the exposures from eq. (3) are also averaged in the axial direction:

$$\overline{E^m} = \frac{\sum_k E_k^m \cdot \Delta z_k}{H} \tag{7}$$

with

$$H = \sum_k \Delta z_k \tag{8}$$

The cross sections of each material are now determined from the interpolation formulas:

$$\overline{\Sigma^{am}} = \Sigma^m (F, \overline{E^m}) \tag{9}$$

Finally, they are again averaged over the materials:

$$\overline{\Sigma^{x}} = \frac{\sum_{m} \overline{\Sigma^{am}} \cdot V^{m}}{\sum_{m} V^{m}} \qquad (10)$$

Since the cross sections at core average variable values are independent on the power distribution, eq. (7)-(10) are evaluated only once, outside the power iteration.

The above averaging procedure (eq. (5)-(10)) is used for absorption, production, fission, scattering, and transport cross sections. The diffusion coefficient of each axial node is computed from the transport cross section after the final averaging (eq. (6)). The axial reflectors are assumed to consist of a single material per node level (i.e. they are homogeneous in the horizontal directions). Their cross sections depend only on boron concentration and water temperature. No averaging is therefore needed; the cross sections are determined from the interpolation formulas using the same fixed variable values as in the core.

If the dependence of the cross sections on power and exposure were linear, the averaging scheme of eq. (3)-(6) would produce the same results as a volume-weighted average over each axial node level of the three-dimensional configuration. For fuels without burnable poisons a linear function is a reasonable approximation to the exposure dependence of the cross sections, and since the influence of the power on the cross sections is usually small, we do not commit a great error in assuming a linear dependence on the power.

3.3 Flux and Power Calculation

The axial flux distribution is calculated by means of a one-dimensional version of the nodal coarse-mesh diffusion method used in SEXI (4). This method uses analytical solutions of the neutron diffusion equation, i.e. exponentials and trigonometric functions, as expansion functions of the flux within a node. Neighbouring nodes are coupled by means of the continuity of the partial currents. This method is restricted to two energy groups.

The power density (in MW/ton) is calculated from the fluxes in each node by means of the formula:

$$P_k = \frac{Q_k \cdot \sum_g \Sigma_{fgk} \cdot \phi_{gk}}{\bar{\rho}} \qquad (11)$$

The fission cross sections Σ_f and the energy per fission Q are computed and averaged over the radial directions according to the formulas of the previous section. $\bar{\rho}$ is the average (smeared) uranium density in the core. The powers per axial node are then normalized to an average of $\bar{P}$ (i.e. the core average power density determined from the input for the two-dimensional calculation).

3.4 Bucklings and k-eff Correction

After the flux and power calculation has converged, the axial bucklings (per energy groups) and the k-eff correction due to the difference between flux-weighted cross sections and cross sections at core average variable values are determined.

The bucklings are defined so that the axial leakage from the one-dimensional calculation is preserved. We assume the area of each boundary surface of the 1-D configuration to be unity, then the volume is equal to the height H and the leakage can be represented by:

$$L_g = \overline{D_g} B_g^2 \overline{\phi_g} H \qquad (12)$$

On the other hand, the axial leakage can be expressed as the sum of the net outgoing currents J^{net} at the bottom and top core boundaries:

$$L_g = J_{gb}^{net} + J_{gt}^{net} \qquad (13)$$

where the indices b and t stand for bottom and top, respectively. The net outgoing currents are computed as the difference of the outgoing and incoming partial currents, which are known from the flux calculation (see section 3.3)

Equating (12) and (13) and solving for the buckling results in:

$$B_g^2 = \frac{J_{gb}^{net} + J_{gt}^{net}}{\overline{D_g}\ \overline{\phi_g}\ H} \qquad (14)$$

The average diffusion coefficient $\overline{D_g}$ is computed from the average transport cross section (i.e. 1/3 D) which is determined with

flux-volume weighting:

$$\overline{D_g} = \frac{\sum_k \phi_{gk} \Delta z_k}{\sum_k \frac{\phi_{gk} \Delta z_k}{D_{gk}}} \qquad (15)$$

In the denominator of formula (15) the multiplication and division by 3 have been omitted because they cancel each other. The numerator in (15) is equal to $\overline{\phi_g}$ H and the final formula for the buckling becomes:

$$B_g^2 = \frac{J_{gb}^{net} + J_{gt}^{net}}{(\sum_k \phi_{gk} \Delta z_k)^2} \cdot \sum_k \frac{\phi_{gk} \Delta z_k}{D_{gk}} \qquad (16)$$

For the determination of the eigenvalue correction flux-volume weighted absorption, production, and scattering cross sections as well as the values of these cross sections at core average variable values are needed. The latter cross sections have already been defined (eq. (7)-(10)), the former are computed according to the formula

$$\overline{\Sigma^f} = \frac{\sum_k \Sigma_k \phi_k \Delta z_k}{\sum_k \phi_k \Delta z_k} \qquad (17)$$

where the cross sections Σ_k are those from eq. (6). The k_∞, i.e. the multiplication factor for an infinite medium, can be calculated from the two-group macroscopic cross sections (since the flux calculation method used works only in two groups we can restrict ourselves to two groups here too) as follows: The neutron balance equations for an infinite medium with a general fission spectrum (but

normalized to a sum of unity) and upscattering are:

$$\begin{aligned}(\Sigma_{a1} + \Sigma_{1\to2})\phi_1 &= \Sigma_{2\to1}\,\phi_2 + \frac{\chi_1}{k_\infty}\,(\nu\Sigma_{f1}\,\phi_1 + \nu\Sigma_{f2}\,\phi_2)\\ (\Sigma_{a2} + \Sigma_{2\to1})\phi_2 &= \Sigma_{1\to2}\,\phi_1 + \frac{\chi_2}{k_\infty}\,(\nu\Sigma_{f1}\,\phi_1 + \nu\Sigma_{f2}\,\phi_2)\end{aligned} \tag{18}$$

Reordering of eqs. (18) results in:

$$\begin{aligned}&(\Sigma_{a1} + \Sigma_{1\to2} - \frac{\chi_1}{k_\infty}\,\nu\Sigma_{f1})\phi_1 - (\Sigma_{2\to1} + \frac{\chi_1}{k_\infty}\,\nu\Sigma_{f2})\phi_2 = 0\\ &-(\Sigma_{1\to2} + \frac{\chi_1}{k_\infty}\,\nu\Sigma_{f1})\phi_1 + (\Sigma_{a2} + \Sigma_{2\to1} - \frac{\chi_2}{k_\infty}\,\nu\Sigma_{f2})\phi_2 = 0\end{aligned} \tag{19}$$

Eqs. (19) are a homogeneous linear system for the fluxes ϕ_1 and ϕ_2. A non-trivial solution for the fluxes exists only if the determinant of the system vanishes. From this condition, k_∞ can be determined:

$$k_\infty = \frac{(\chi_2\,\Sigma_{a1} + \Sigma_{1\to2})\nu\Sigma_{f2} + (\chi_1\,\Sigma_{a2} + \Sigma_{2\to1})\nu\Sigma_{f1}}{\Sigma_{a1}\,\Sigma_{a2} + \Sigma_{a1}\,\Sigma_{2\to1} + \Sigma_{a2}\,\Sigma_{1\to2}} \tag{20}$$

With the cross sections from eq. (10) and (17) we obtain two different values for the core average k_∞, viz.

$$\overline{k^a} = k_\infty\,(\overline{\Sigma^a}) \tag{21}$$

with the cross sections computed at core average variable values (eq. (7)-(10)), and

$$\overline{k^f} = k_\infty\,(\overline{\Sigma^f}) \tag{22}$$

with the flux-volume weighted cross sections. The k-eff of the reactor is assumed to be proportional to the average fuel k_∞. Therefore, the relative k-eff correction (i.e. the effect of the

difference between $\overline{k^a}$ and $\overline{k^f}$ on k-eff) is equal to the relative difference Δ of the two average k_∞ values,

$$\Delta = \frac{\overline{k^a} - \overline{k^f}}{\overline{k^a}} \qquad (23)$$

As explained in chapter 2, $\overline{k^a}$ is normally greater than $\overline{k^f}$, therefore Δ is positive. If the multiplication factor for a given boron concentration is determined in the two-dimensional calculation, the user should multiply the result for k-eff by $(1-\Delta)$ to account for the effect of the simplified axial averaging of the cross sections. If the critical boron concentration is searched for in the 2-D calculation, the program edjusts the critical eigenvalue (i.e. the target k-eff for the poison density iteration) according to the formula:

$$k^* = \frac{k_{crit}}{1-\Delta} \qquad (24)$$

In eq. (24) k_{crit} is the critical eigenvalue defined by input (it can be different from unity e.g. to compensate a bias known from previous calculations) and k^* is the target multiplication factor for the boron concentration search at the present time point.

3.5 Program Organization

The methods described in sections 3.2-3.4 have been introduced as a module, called AXBUCK, into the EIR light water reactor simulation code SILWER (1). The global organization of SILWER and the position of AXBUCK within the code are shown in Figure 2. Each of the modules in Figure 2 can be skipped if the user chooses to do so. A typical SILWER calculation (a time point of a reactor cycle calculation) runs as follows: First, the exposure distribution is updated using the power distribution from the previous calculation; in a two-dimensional calculation with axial calculation both the two- and three-dimensional exposure distributions (see section 3.2) are determined. The axial calculation (if selected by the user) is performed directly after BURNUP, before the iterations of the 2-D calculation. Since the cross sections depend on power and water temperature and the temperature distribution depends on the power distribution, an iteration between power, temperature, cross sections, and neutron fluxes is required. SILWER has thermohydraulics modules for PWR's and BWR's (5). In 2-D calculations these modules, which work only for configurations with more than one node in the axial direction, are skipped. After the thermohydraulic calculation the cross sections of each node are determined from the interpolation formulas. Two nodal programs are available for the flux calculation: SEXI (4) and NODLEG (6). The former uses an analytical method and is restricted to two energy groups, the latter is based on a polynomial method and can be used for an arbitrary group number. If the boron concentration or the control rod position for which the multiplication factor k-eff of the reactor reaches a prescribed value are to be

determined, the appropriate parameter is adjusted in the SEARCH module. In a 2-D calculation with axial calculation the target k-eff for the poison density search is determined from eq. (24), else it is equal to the input critical eigenvalue. Finally the power distribution in the core is computed and normalized to the input total power; after this, the calculation returns to the thermohydraulics (or the cross section interpolation) module. After this power-thermohydraulics iteration has converged or the maximum number of iterations (given by input) has been reached, the results are printed out. They can also be stored on disk and used as restart values for a subsequent calculation.

The flow chart of the AXBUCK module is shown in Figure 3. The organization of AXBUCK is similar to that of SILWER in the sense that an iteration between cross sections and power distribution has to be performed. However, there is no thermohydraulic calculation in AXBUCK (in the present version) and the boron concentration is not modified in the axial calculation even if the critical poison density is searched for in the 2-D calculation. Since the shape of the axial flux distribution is almost independent on the boron concentration, the main results of the axial calculation, i.e. the bucklings and the k-eff correction, are hardly influenced by this parameter. The first step of the axial calculation is the radial averaging of the exposures per material (eq. (3)). This operation and the determination of the cross sections at core average variable values (eq. (7)-(10)) are performed before the power iteration. The initial flux and power distributions for the start of the iterations are taken from a previous calculation or, if no such distributions are available,

assumed to be flat throughout the one-dimensional configuration (with a power density equal to the core average value in all fuel nodes). As the first step in the power iteration, the cross sections are computed and averaged over the materials according to eq. (5) and (6). Then the one-dimensional flux distribution is calculated, within the flux calculation routine iterations over the flux and the eigenvalue are performed. Finally the axial power distribution is determined according to eq. (11) and fed back to the cross section interpolation. After the multiplication factor and the flux and power distributions have converged, the buckling for each energy group is computed from eq. (16) and the eigenvalue correction is determined according to eq. (20)-(24). The flux and power distributions are stored on disk so that they can be used as initial values for the next time point or a restart calculation.

4. Test Results

The two-dimensional core simulation methods with and without axial calculation were compared to the three-dimensional calculations for a simplified model of a 350 MWel PWR. The main data of this reactor are given in Table IV.

Thermal Power	1130 MW
Number of Fuel Assemblies	121
Uranium Mass	39.2 tons
Average Power Density	28.8 MW/ton
Enrichment of Fresh Fuel	3.5 weight-%
Average Water Temparature	300 degrees C

Table IV Characteristics of the Reactor for Test Calculations

The principal simplifications for the calculations were:

1) No thermohydraulics, i.e. constant water temperature (and density) throughout the core.
2) Only one fuel assembly type, i.e. idealized equilibrium core.
3) Same relative axial exposure distribution for all previously irradiated assemblies at BOC.

Tables of the cross sections of the fuel assemblies as a function of power, exposure, and boron concentration were generated by means of the EIR LWR fuel assembly code BOXER (2, 7) and interpolated by third-order polynomials of these state variables. The group constants

of the reflectors were also determined by BOXER calculations and represented as functions of the boron concentration.

The core average burnup per cycle was assumed to be 9 GWd/ton; at the beginning of the cycle the core consists of 32 fresh fuel assemblies, the same number of assemblies with axially averaged exposures of 7 GWd/ton and 18 GWd/ton, respectively, and 25 assemblies irradiated to 27 GWd/ton (the fuel assemblies are normally discharged after four cycles). The above exposure values are based on the assumption that the fresh assemblies have the lowest powers (because they are located at the core periphery) whereas the assemblies being irradiated in the second cycle have the highest powers. The loading pattern, i.e. the arrangement of the fuel assemblies with different initial exposures in the x-y-plane, and the axial exposure distribution were chosen so that the calculated radial and axial power distributions were similar to those in an actual reactor (8) and the maximum assembly power remained within acceptable limits. For the loading pattern the choice was restricted by the above numbers of assemblies with given exposures and the eighth-core symmetry.

The critical boron concentration was searched for in all SILWER calculations. For the two-dimensional core simulation without axial calculation the buckling was determined from the results of the 3-D calculation at BOC using the average axial power distribution as an approximation to the flux distribution. Since the partial currents at the core boundaries were not known in this approximation, the procedure shown in section 3.4 had to be modified. The net outgoing currents were estimated according to elementary diffusion theory:

$$L = D \cdot \left(\frac{d\phi}{dz}(0) - \frac{d\phi}{dz}(H) \right) \qquad (25)$$

where z=0 and z=H denote the lower and upper core boundaries, respectively, and the cross section area of the configuration has been assumed to be unity like in section 3.4. By equating (25) with (12) we obtain

$$B^2 = \frac{\frac{d\phi}{dz}(0) - \frac{d\phi}{dz}(H)}{\bar{\phi} \cdot H} \qquad (26)$$

The buckling determined from the axial power distribution at BOC and eq. (26) is $1.65 \cdot 10^{-4}$ cm^{-2}, whereas the geometric buckling for an active core height of 304.8 cm and a reflector saving of 7 cm is $9.71 \cdot 10^{-5}$ cm^{-2}. The former buckling was used for all time points.

Table V shows the critical boron concentrations determined by the 3-D calculations and the 2-D calculations without and with axial calculation as a function of burnup.

Burnup (MWd/t)	Critical Boron Concentration (ppm)		
	3-D Calculation	2-D Calculation	
		without Ax. Calc.	with Ax. Calc.
0	783	819	785
1000	656	700	658
2000	534	583	536
3000	416	470	418
4000	302	361	304
5000	193	255	195
6000	88	152	90

Table V Critical Boron Concentrations in 3-D and 2-D Calculations

It can be seen that the accuracy of the 2-D core simulation is significantly improved by the axial calculation: The 2-D calculation with a constant buckling overpredicts the critical boron concentration by 36 to 64 ppm and thia overestimate increases monotonously with burnup, whereas the difference in the case with the axial calculations is only 2 ppm and remains constant during the cycle. These differences can be translated into k-eff differences using the relation that 15 ppm correspond to 0.1% in k-eff (for the cross section set used here): The 2-D calculations without axial calculation overpredict ths k-eff by 0.24 to 0.43%, with the axial calculation tais overestimate reduces to approximately 0.015%. While the former two values are comparable to the target accuracy given in Table I and not satisfactory for a single source of uncertainty (see also chapter 2), the latter value can be neglected. As shown in chapter 2, the 2-D calculation with a constant buckling overpredicts the cycle length (i.e. the burnup at which the critical poison density becomes zero) by 600 MWd/t or 9% (this can also be seen from Table V); in the case with axial calculations this overestimate reduces to 20 MWd/t or 0.3%. The result of the former 2-D calculation does n_t mset the target accuracy for the reactivity lifetime, whereas the result of the latter calculation can be said to be in excellent agreement with that of the 3-D core simulation.

The radial power distributions of the two- and three-dimensional calculations are shown in Figure 4 at the beginning of the cycle and in Figure 5 at an average burnup of 6000 MWd/t. The standard deviations and the maximum relative differences between the powers per assembly of the 2-D and 3-D calculations are summarized in Table VI.

Burnup (MWd/t)	without Axial Calculation		with Axial Calculation	
	Standard Deviation(%)	Maximum Difference(%)	Standard Deviation(%)	Maximum Difference(%)
0	1.1	1.9	0.8	1.5
1000	0.9	1.6	0.5	0.9
2000	0.8	1.6	0.4	0.7
3000	0.8	1.3	0.3	0.4
4000	0.7	1.4	0.1	0.3
5000	0.7	1.2	0.1	0.2
6000	0.6	1.2	0.1	0.2

Table VI Relative Deviations of the Powers per Fuel Assembly of the 2-D Calculations from the Axially Averaged Powers of the 3-D Calculation

It can be seen that the agreement of the power distribution of the 2-D calculation with the 3-D results is somewhat improved by the axial calculation, however all the differences given in Table VI are well within the target accuracy of Table I. It may be noted that the differences in the power distributions between the two- and three-dimensional core simulations decrease more rapidly as a function of burnup if axial calculations are performed. Usually the 2-D calculation predicts higher powers than the 3-D calculation in the core centre and lower values at the periphery (see Figure 4). In the case with axial calculations, however, the signs of these differences change at 5000 to 6000 MWd/t (Figure 5); therefore it is possible that the magnitude of the differences would increase somewhat at higher burnups.

The power distribution from the axial calculation and the average axial power distribution of the 3-D calculation at the beginning of the cycle are compared in Table VII.

Axial Core Node (1=Bottom)	Relative Power		Relative Difference in % $\left(\frac{\text{Ax.-3-D}}{\text{3-D}}\right)$
	3-D Calculation (Average)	Axial Calculation	
1	0.457	0.455	-0.4
2	0.813	0.809	-0.5
3	1.031	1.028	-0.3
4	1.135	1.135	0.0
5	1.170	1.171	+0.1
6	1.170	1.173	+0.3
7	1.162	1.165	+0.3
8	1.157	1.161	+0.3
9	1.161	1.165	+0.3
10	1.168	1.171	+0.3
11	1.166	1.168	+0.2
12	1.130	1.130	0.0
13	1.024	1.022	-0.2
14	0.804	0.800	-0.5
15	0.450	0.448	-0.4

Table VII Axial Power Distributions (Normalized to an Average of 1) of 3-D and Axial Calculations at BOC

The differences observed in this table are representative of the whole cycle: In the axial calculation the power is lower than in the 3-D calculation at the lower and upper core edges and higher in the middle of the core. The standard deviations are between 0.2% and 0.4% and the maximum differences do not exceed 0.6%.

The bucklings and the relative k-eff correction from the axial calculation are shown in Table VIII.

Burnup (MWd/t)	Bucklings (cm^{-2})		Relative k-eff Correction Δ^* (%)
	Group 1	Group 2	
0	$1.87 \cdot 10^{-4}$	$-2.23 \cdot 10^{-4}$	0.31
1000	$1.97 \cdot 10^{-4}$	$-2.45 \cdot 10^{-4}$	0.32
2000	$2.06 \cdot 10^{-4}$	$-2.68 \cdot 10^{-4}$	0.33
3000	$2.15 \cdot 10^{-4}$	$-2.91 \cdot 10^{-4}$	0.34
4000	$2.23 \cdot 10^{-4}$	$-3.14 \cdot 10^{-4}$	0.35
5000	$2.31 \cdot 10^{-4}$	$-3.37 \cdot 10^{-4}$	0.35
6000	$2.39 \cdot 10^{-4}$	$-3.60 \cdot 10^{-4}$	0.35

* Definition of Δ see eq. (23)

Table VIII Bucklings and k-eff Correction from the Axial Calculations

The buckling in the second (thermal) group is negative because the number of thermal neutrons entering the core from the reflector is greater than the number of those leaving the core. The bucklings can be averaged over the energy groups by weighting them with flux and diffusion coefficient:

$$\overline{B^2} = \frac{\overline{D_1}\,\overline{\phi_1}\,B_1^2 + \overline{D_2}\,\overline{\phi_2}\,B_2^2}{\overline{D_1}\,\overline{\phi_1} + \overline{D_2}\,\overline{\phi_2}} \qquad (27)$$

Since the product of flux and diffusion coefficient for group 1 exceeds that for group 2 by a factor of about 15, the average buckling is always positive and increases monotonously with the burnup. At the beginning of the cycle the average buckling is $1.61 \cdot 10^{-4}$ cm^{-2}, this value is consistent with the $1.65 \cdot 10^{-4}$ cm^{-2} determined from the average axial power distribution at BOC (see above). The effect of the flattening of the axial power distribution during the cycle on the leakage is clearly reflected by the increase of the bucklings in Table VIII. The last column in this table shows that the difference between

the k_∞ values from flux-volume weighted cross sections and from cross sections at axially averaged variable values is almost constant during the cycle and that the estimate of 0.3% given for this effect in chapter 2 (on a simple basis) was correct.

The computing time for a typical time point on a CDC 6400 is 14 seconds in the 2-D calculation (including the axial calculation) and 140 seconds for the 3-D core simulation. The computing cost depends also on the input/output (IO)-time (data transfer between central memory and disk storage) and the core memory used; however these quantities are more installation specific and therefore not given explicitly. On the computer used at EIR the cost of the 3-D calculation is approximately 6 times that of the 2-D calculation. The cost ratio is smaller than that of the CP times because the ratio of the IO-times is only about 3. The axial calculation, including the determination of the three-dimensional exposure distribution, requires 1.5 seconds computing time or approximately one tenth of the time of the 2-D calculation. Since the axial calculation needs little data transfer between central memory and disk its contribution to the computing cost is even smaller: The cost of the axial calculation is only 6% of that of the 2-D calculation.

5. Conclusions

For an accurate determination of the multiplication factor or the critical boron concentration in two-dimensional PWR core calculations the increase of the axial leakage due to the flattening of the axial power distribution and the effect the difference between the cross sections determined for average values of the state variables and flux-volume weigbted cross sections must be taken into account. The axial calculation method presented in this report provides an efficient tool to solve this problem. The radial cross section averaging is performed with simplified procedures which help to keep the computing cost low, but the axial calculation in the one-dimensional configuration is carried out with the same degree of sophistication as the actual core simulation.

The results of the test example presented here show that the axial calculation improves the agreement of the critical boron concentrations between two- and three-dimensional calculations by more than an order of magnitude: The overestimate of the critical poison density in comparison to the three-dimensional calculation is reduced from some 50 ppm (averaged over the cycle) to only 2 ppm, which corresponds to 0.015% in k-eff and can be neglected. Moreover, the two-dimensional core simulation overpredicts the cycle length considerably (by 9% in the present example) if the axial buckling is kept constant. If the axial calculation method is used, this quantity, which is important for the economy of the plant operation, agrees almost perfectly with the result of the 3-D calculation. The differences between the radial power distributions of the two- and three-dimensional core simulations are somewhat reduced by the axial

calculation although the agreement is quite satisfactory for both versions of the two-dimensional calculation. The average axial power distribution of the three-dimensional calculation is well reproduced by the axial calculation. All these improvements are achieved with an increase of the computing time of the two-dimensional calculation of approximately one tenth and an even smaller increase of the computing cost.

However, the above good results were obtained for a somewhat simplified model of a pressurized water reactor. The effect of neglecting the spatial variation of the water temperature and density and the performance of the methods described here in more heterogeneous cores, e.g. with different fuel assembly types, remain to be checked. The final validation of these methods (and of the whole EIR LWR code system) will be core follow calculations of actual PWR operating cycles.

Acknowledgements

The author is indebted to J.M. Paratte for useful suggestions and valuable discussions and to C. Maeder for the support in the programming, especially for providing the flux calculation routine.

References

(1) C. Maeder et al.

Calculations with the EIR Light Water Reactor Code System. Proceedings of the NEA/OECD Conference on Calculations of 3-Dimensional Rating Distributions in Operating Reactors, Paris, November 1979, p.181

(2) K. Foskolos, P. Grimm, C. Maeder, J.M. Paratte

Qualification des méthodes LWR-EIR pour l'évaluation des bassins compacts

EIR-Report 497 (1983)

(3) Reactor Burnup Physics

Proceedings of an IAEA panel, Vienna, July 12-16, 1971, p. 278

(4) M. Makai, C. Maeder

A Fast Nodal Neutron Diffusion Method for Cartesian Geometry

Nuclear Science and Engineering, 84, 390 (1983)

(5) K. Foskolos, S. Guentay, G. Varadi

Die Core-Thermohydraulik-Moduln des LWR-Simulationscodes SILWER

EIR-Report 452 (1982)

(6) C. Maeder

A Nodal Diffusion Method with Legendre Polynomials

ANS-Meeting, Gatlinburg, April 1978, Conf-780401, p. 121

(7) C. Maeder, J.M. Paratte

Calculation of LWR Fuel Elements Containing Burnable Poison and Plutonium

TANS-20, 359, 1975

(8) I.H. Gibson, G. Nash, R.E. Mott, S. Rizvi

The Performance of UK Coarse Mesh PWR Calculations in Comparison with Reactor Data.

Proceedings of the NEA/OECD Conference on Calculations of 3-Dimensional Rating Distributions in Operating Reactors, Paris, November 1979, p. 17

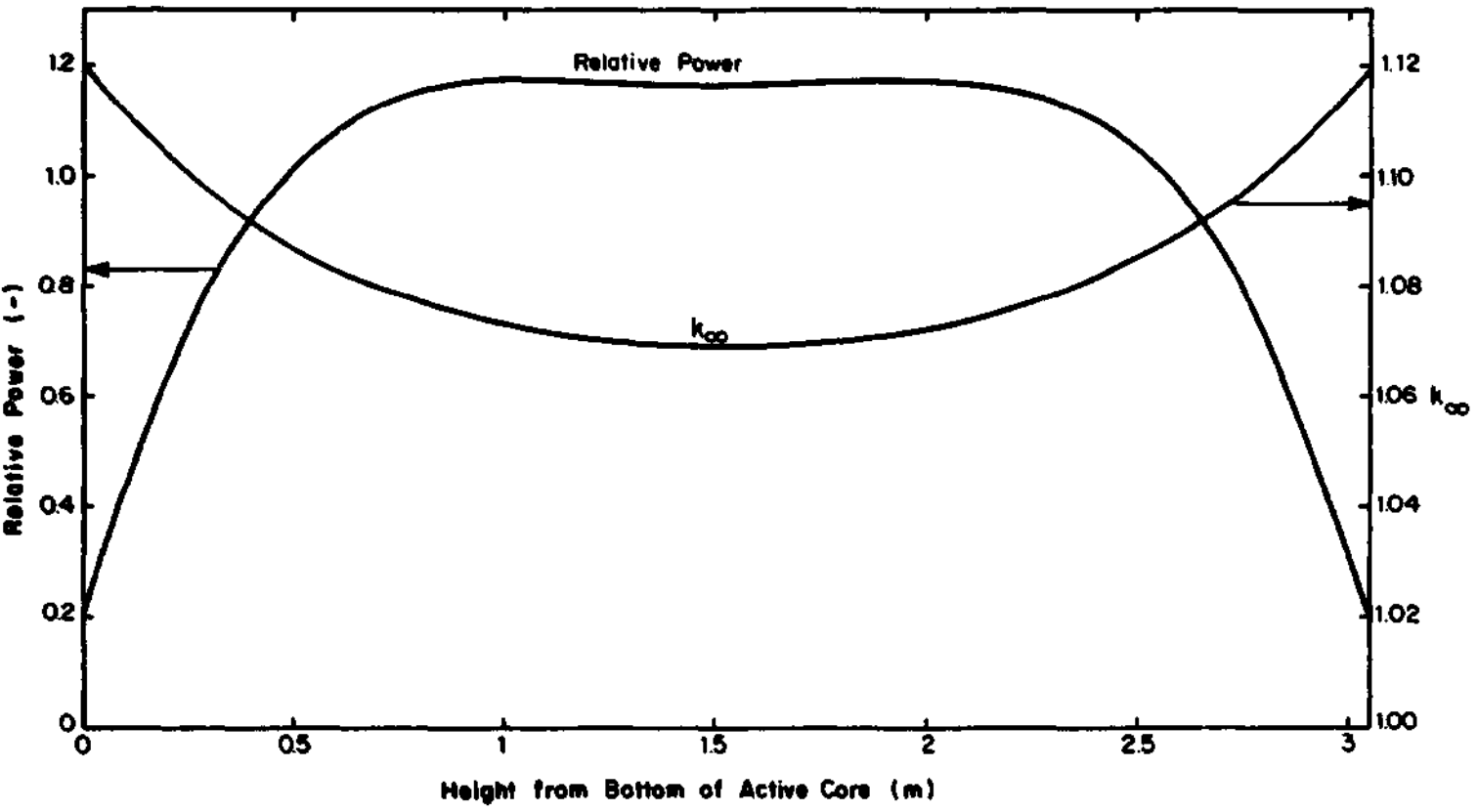

Figure 1 : Average Axial Power and k_{∞} Distribution at BOC (from 1-D Calculation)

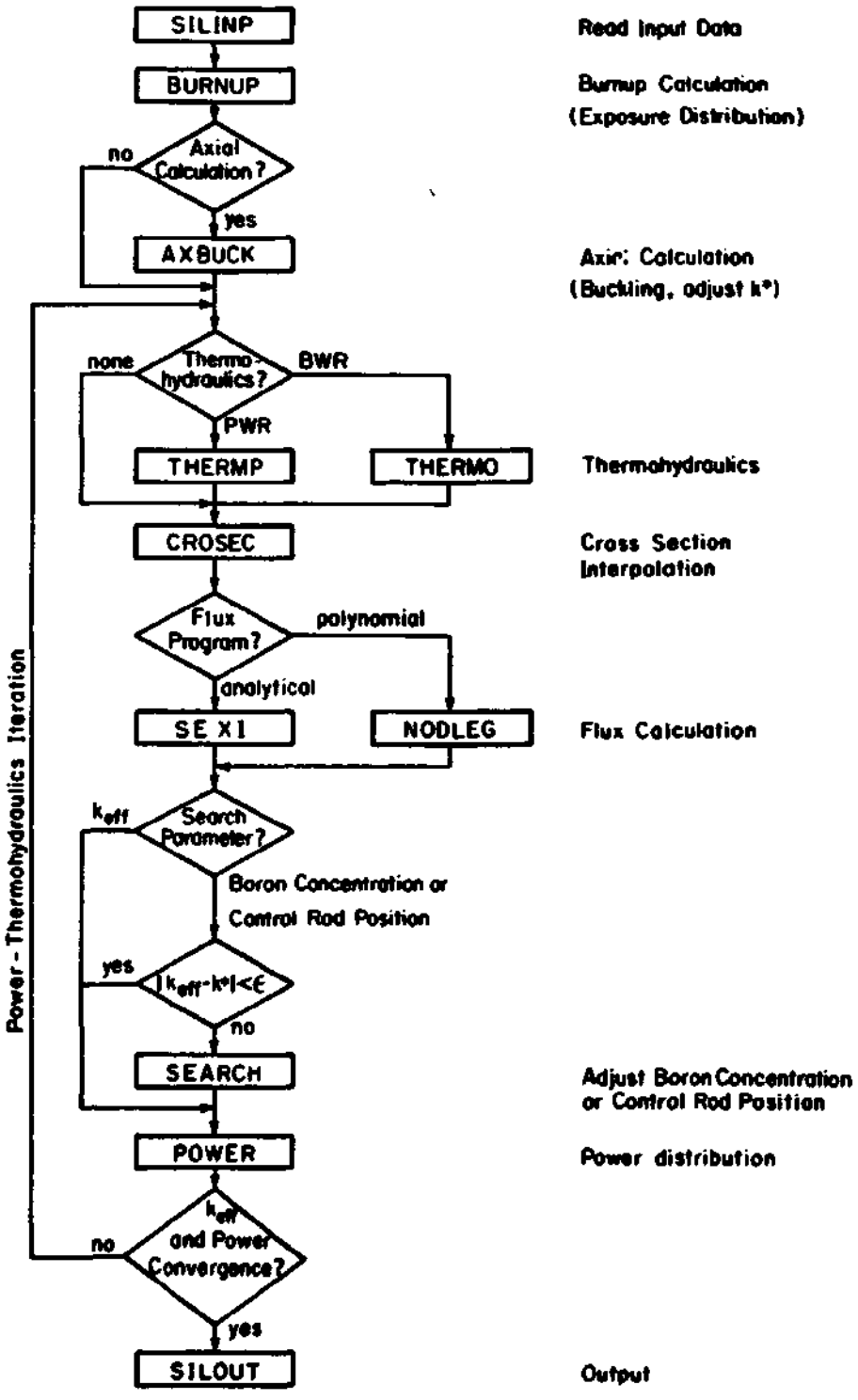

Figure 2: SILWER Flow Chart (simplified)

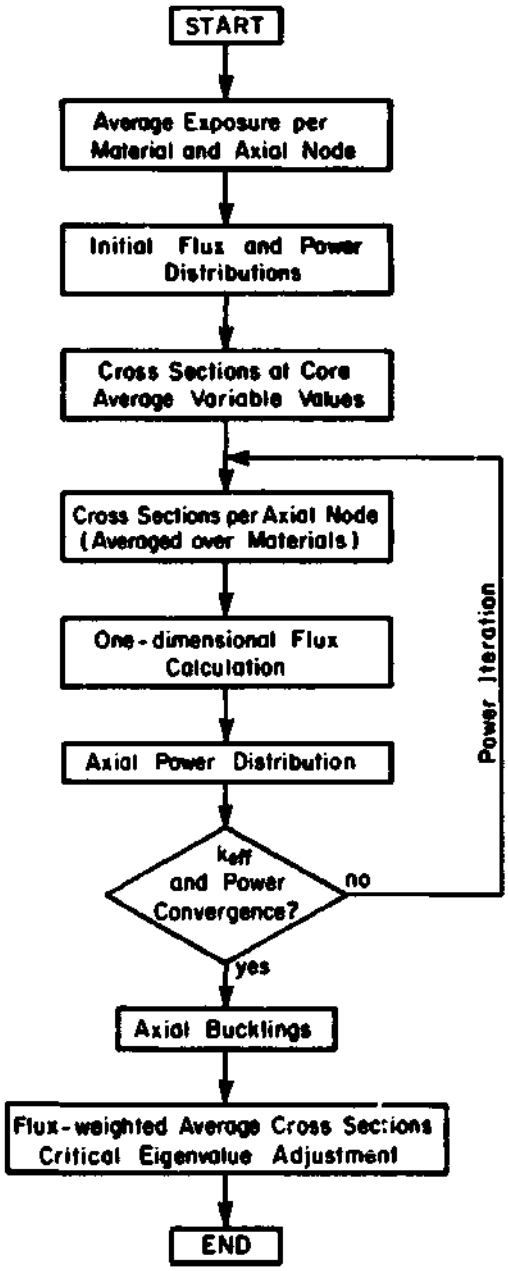

Figure 3: AXBUCK Flow Chart

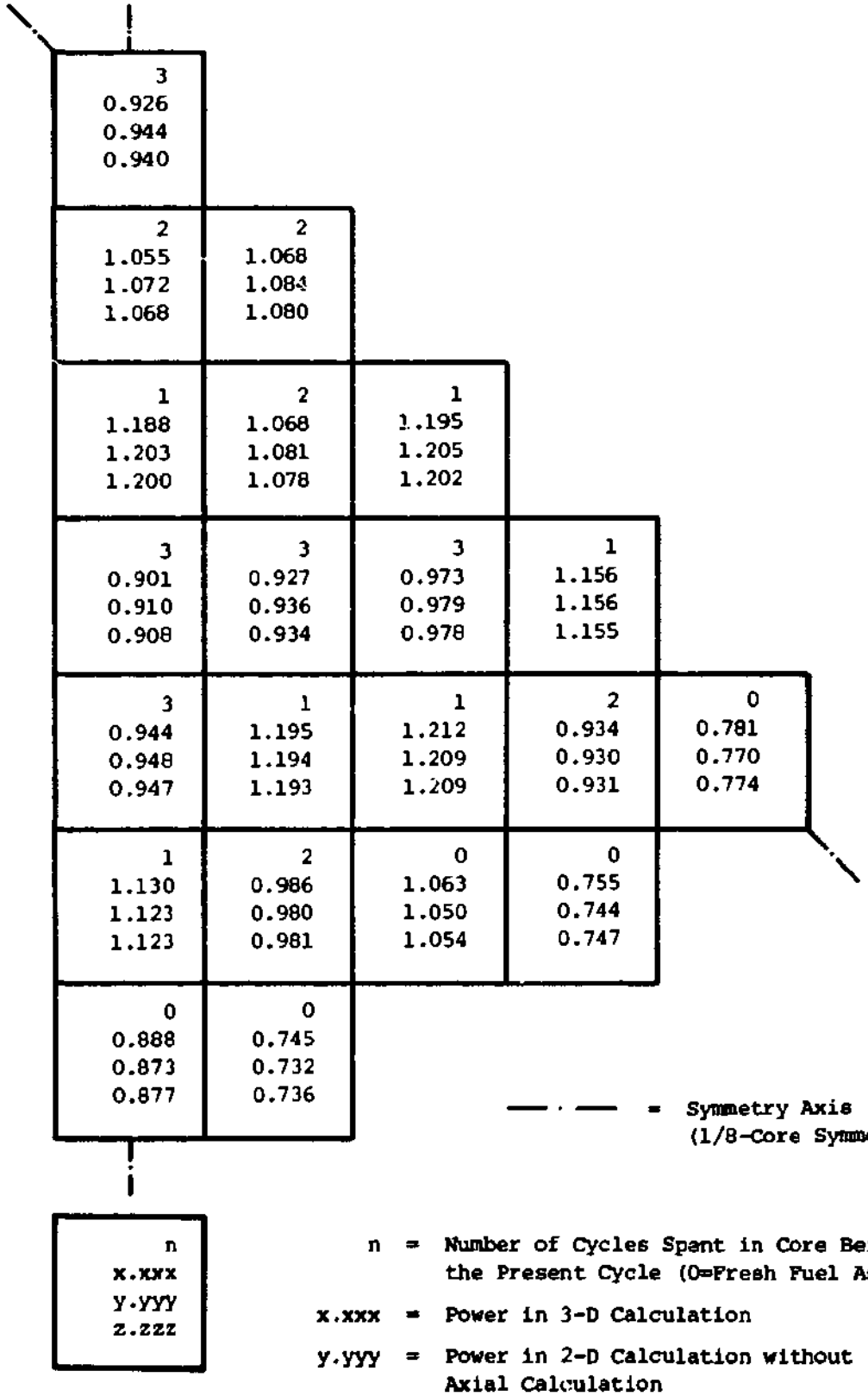

Figure 4: Radial Power Distributions (Normalized to an Average of 1) of Two- and Three-Dimensional Calculations at the Beginning of the Cycle

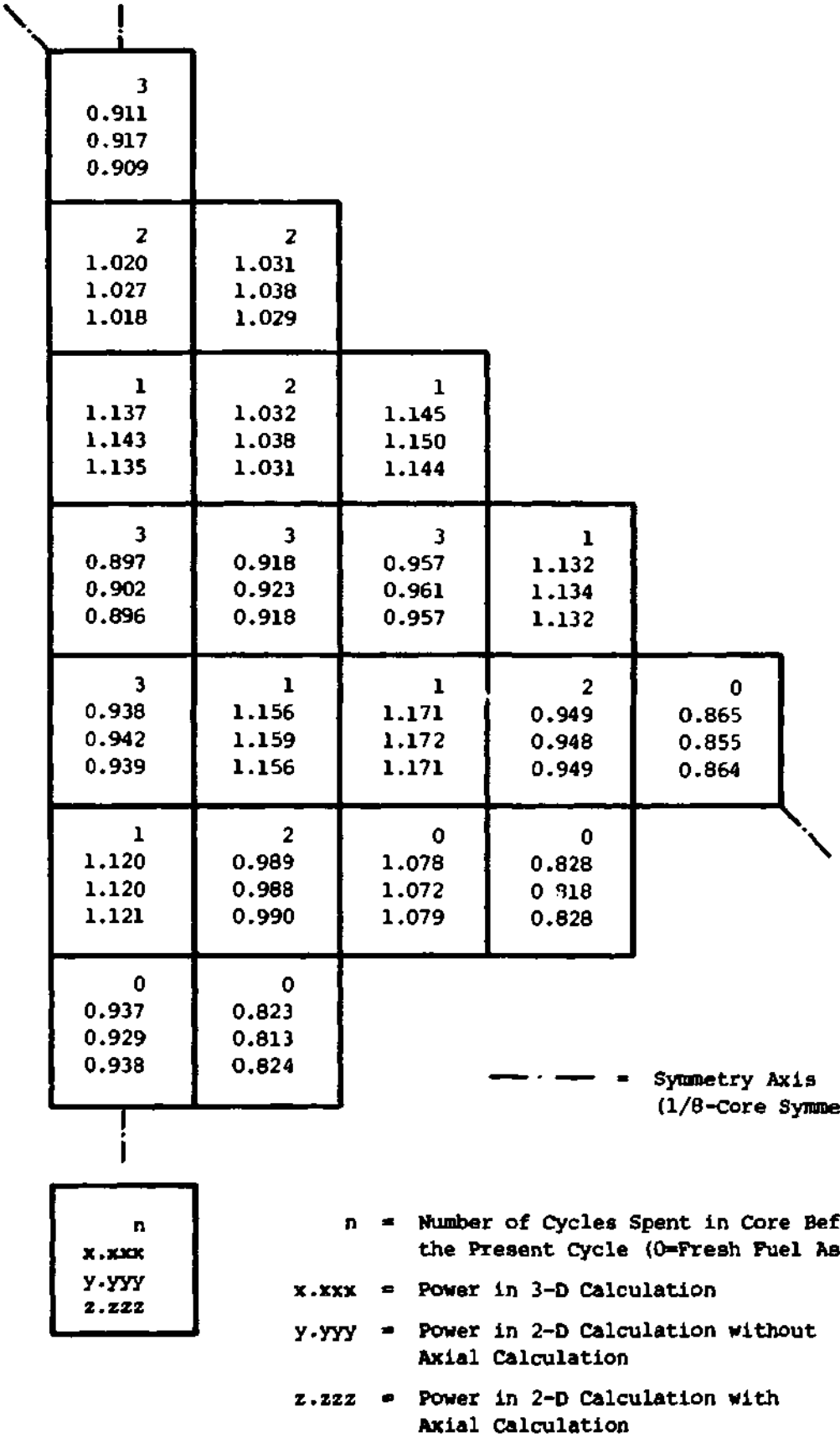

Figure 5: Radial Power Distributions (Normalized to an Average of 1) of Two- and Three-Dimensional Calculations at an Average Burnup of 6000 MWd/t